Transition between Tamm-like and Shockley-like surface states in optically induced photonic superlattices

Natalia Malkova,[1,2] Ivan Hromada,[1] Xiaosheng Wang,[1] Garnett Bryant,[2] and Zhigang Chen[1,3]
[1]*Department of Physics and Astronomy, San Francisco State University, San Francisco, California 94132, USA*
[2]*National Institute of Standards and Technology and Joint Quantum Institute, University of Maryland, Gaithersburg, Maryland 20899, USA*
[3]*The Key Laboratory of Weak-Light Nonlinear Photonics, Ministry of Education and TEDA Applied Physics School, Nankai University, Tianjin 300457, China*
(Received 3 August 2009; published 8 October 2009)

We study the formation of Shockley-like surface states and their transition into Tamm-like surface states in an optically induced semi-infinite photonic superlattice. While perfect Shockley-like states appear only when the induced superlattice with alternating strong and weak bonds is terminated properly with an unperturbed surface, deformed Shockley-like surface states often appear in the so-called inverted band gap when the surface perturbation is nonzero. Furthermore, transitions between linear Tamm-like, Shockley-like, and nonlinear Tamm-like surface states are also observed by fine tuning the surface perturbation. Using coupled-mode theory, we confirm the existence of these linear and nonlinear surface states in a finite array of N identical single-mode waveguides coupled with alternating strong and weak bonds.

DOI: 10.1103/PhysRevA.80.043806 PACS number(s): 42.65.Tg, 78.68.+m

Localized surface waves are found everywhere in nature, from electronic Tamm [1] and Shockley [2] surface states to liquid-helium surface electrons [3], acoustic surface waves [4], and plasmon-polariton waves tightly bound to metal surfaces [5]. In condensed-matter physics, for example, electronic surface states have served as a paradigm for studying fundamental issues in two-dimensional electronic systems involving electron-electron, electron-phonon interactions in solids and the effect of atomic spin-orbit interaction on the formation of spin-polarized surface states important in spintronics [6]. Even though Tamm and Shockley surface states were predicted in early 1930s [1,2], it was not possible for decades to demonstrate such states in the pure form that Tamm and Shockley originally investigated in theoretically [7]. Then, the technological development of superlattice (SL) fabrication provided an ideal platform to study electronic surface waves. Indeed, it was in a semiconductor SL that Tamm states were first observed [8]. Since then, surface phenomena have been studied extensively with SLs driven by both fundamental interests and practical applications.

An interesting and subtle issue is the difference between Tamm-like surface states (TSs) and Shockley-like surface states (SSs). TSs arise from an asymmetrical surface potential and the formation of such surface states requires exceeding a threshold perturbation of the surface potential. On the other hand, SSs result from the crossing of atomic orbitals [2] or the crossover of adjacent bands. Two characteristic properties of SSs are that, in contrast to TSs, SSs can exist without a surface perturbation and the degree of localization of the surface modes depends on the width of the gap between the energy bands. While this difference stimulated a great deal of theoretical interest, the demonstration of Shockley versus Tamm electronic states has been a challenge for experimentalists because of the intrinsic defects in and complicated nature of real surfaces.

In the field of optics, surface electromagnetic wave propagation is a problem of history as venerable as that in condensed-matter physics [9]. Despite the earlier theoretical prediction and experimental observation of linear optical surface waves in periodic layered media [10], most researches have focused on the study of nonlinear optical surface waves [11,12]. This is because in most cases, optical surface waves cannot exist under linear conditions at the surface of dielectric media, whereas under nonlinear conditions their existence simply requires high power. Recently, nonlinear optical surface waves in the form of discrete surface solitons have been successfully demonstrated in a number of experiments [13–16]. This was done using a small controllable index contrast in a semi-infinite waveguide array or optically induced photonic lattice. Under self-focusing (self-defocusing) nonlinearity, the light itself is used to induce a positive (negative) surface defect in an otherwise uniform periodic structure thereby achieving surface bound states as discrete in-phase ("staggered" out-of-phase) surface solitons [12–17]. A key feature of the optical surface waves studied so far is that they exist only above a certain threshold. In the *linear* case, surface waves appear only when the contrast of the dielectric constants between the periodically layered and uniform medium, or the perturbation of the dielectric constant for the surface layer, reaches a critical value [10]. In the *nonlinear* case, all surface waves exist only above a power threshold, which determines the light-induced index perturbation at the surface. This suggests that all surface states observed previously in optics have the same physical origin as Tamm states in crystals. On the other hand, linear SSs have been predicted to exist in specially designed defect chains in complex photonic crystal structures [18], but they have never been observed in optical systems until our recent successful demonstration in optically induced photonic SLs [19]. Meanwhile, surface states that do not belong to the family of Tamm states or Shockley states have also been demonstrated as a new type of defect-free surface states in fs-laser-induced curved waveguide arrays [20].

In this paper, we study both experimentally and theoreti-

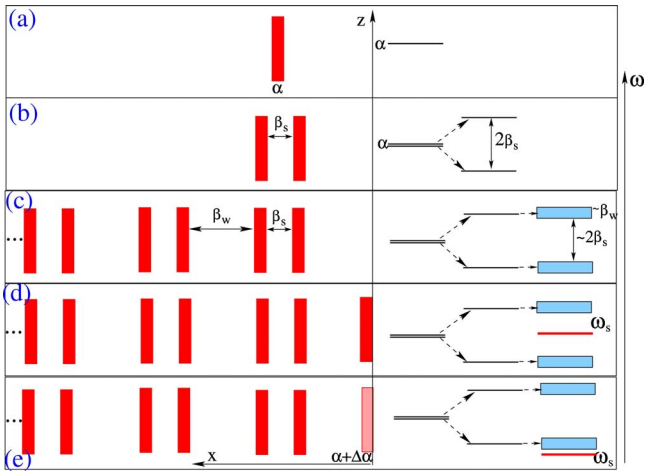

FIG. 1. (Color online) An intuitive explanation of formation of different surface states in superlattices. The left side of each panel illustrates the physical arrangement of single-mode waveguide(s) shown by red vertical stripes. The right side illustrates the corresponding frequency spectrum. (a) Only one waveguide. (b) Two strongly coupled waveguides. (c) A SL consisting of strongly and weakly coupled waveguides terminated at a weak bond. The blue horizontal stripes shown in the right side correspond to the allowed bands. No surface mode exists in this case. (d) A SL terminated at a strong bond and the red horizontal line in spectrum corresponds to the Shockley-like surface mode. (e) A SL terminated at a strong bond with surface perturbation and the red line in spectrum corresponds to the Tamm-like surface mode.

cally the transition between Tamm-like and Shockley-like surface states in an optically induced photonic SL by fine tuning the index perturbation at the interface between the SL and the homogeneous region inside a nonlinear crystal. The induced SL is a waveguide array with alternating strong and weak couplings between waveguides. We show that SSs, observed only when the SL is terminated appropriately, can be transformed into TSs of different types either by intentionally introducing a surface defect (linear scheme) or by increasing the optical power of a probe beam (nonlinear scheme). Specifically, we demonstrate that a surface probe beam can evolve from linear TSs to linear SSs and to nonlinear TSs under different surface conditions. In addition, "imperfect" or "deformed" SSs with characteristic phase distributions are also observed during these transitions. Our experimental observations are in good agreement with our theoretical analysis using coupled-mode theory.

Before describing the details of the aforementioned Tamm-Shockley transition, let us start with a simple question: Why would different terminations of the SL lead to different surface phenomena? To answer this question, we refer to Fig. 1 to first present an intuitive physical picture, where the left panels illustrate the physical arrangement of waveguides shown by the red stripes and the right panels illustrate the corresponding frequency spectrum of the waveguide modes. For the sake of simplicity, let us assume that each waveguide contains a single mode with an eigenvalue α as shown in Fig. 1(a). We refer to the strong and weak couplings between neighboring waveguides as strong bond (SB) and weak bond (WB), respectively, as indicated by the coupling constants β_s and β_w ($\beta_s \gg \beta_w$). Coupling between two waveguides separated by a SB results in splitting the degenerate mode α as shown in Fig. 1(b). If a SL consisting of N unit cells is terminated at a WB [meaning a weak bond is cut as shown in Fig. 1(c)], the weak coupling between the N pairs of strongly coupled waveguides splits each of the two levels into the two allowed bands of width $\sim\beta_w$. These narrow bands are separated by a large gap (the so-called inverted band gap [2] as we shall discuss below) with a width $\sim 2\beta_s$. No localized modes can appear in the gap in this case. On the other hand, if a SL is terminated at a SB, one weakly coupled waveguide exists at the end as shown in Fig. 1(d). The eigenvalue α of this surface waveguide resides exactly in the middle of the band gap, leading to a localized surface mode $\omega_s \approx \alpha$ as shown in the right panel of Fig. 1(d). Without the need of surface perturbation, this surface mode has similar origins as electron Shockley states [2,19]. When there is an additional index perturbation Δn on the surface waveguide, its eigenvalue can change to $\alpha_s = \alpha - \Delta\alpha$. If $\Delta\alpha \geq \beta_s$, the surface mode can move out of the inverted band gap. Especially, if $\Delta\alpha \geq \beta_s + \beta_w$, another surface mode appears with its eigenvalue crossing the allowed band and falling into the lower noninverted band gap as illustrated in Fig. 1(e). This surface mode forms only when the surface perturbation is above a critical value (i.e., $\Delta\alpha \geq \beta_s + \beta_w$), thus, it must be classified as a Tamm-like surface mode. Likewise, the eigenvalue can also change to $\alpha_s = \alpha + \Delta\alpha$ with $\Delta\alpha \geq \beta_s + \beta_w$ and a similar Tamm-like surface mode appears in the upper band gap. Therefore, by modifying the surface perturbation, it is possible to control the transitions between Tamm- and Shockley-like surface modes at ease.

Our experimental setup for creating the SLs with desired surface terminations uses the optical induction technique [21–24]. In our optical induction process, two ordinarily polarized partially coherent beams, each passing through an amplitude mask [23,24], are used to provide two one-dimensional (1D) periodic intensity patterns with 20 μm and 40 μm spacings. Superimposition of the two intensity patterns appropriately leads to a biperiodic intensity pattern. This intensity pattern is used to induce a SL by the photorefractive effect with an interface terminated either at a SB or a WB [Fig. 2(b)]. The experimental challenge is not only to create such SL structures, but also to maintain an invariant interface between the SL and the homogeneous regime across the crystal with the desired SB or WB termination. To do that, the Talbot effect is first eliminated by spatial filtering at the Fourier plane [24] and then the lattice-inducing beams are launched laterally through the short dimension (5 mm) of a strontium barium niobate (SBN) crystal while the probe beam is launched along the orthogonal long dimension (10 mm) of the crystal [see Fig. 2(a)]. Such arrangement ensures that the lattice pattern and the interface remain nearly unchanged along the path of the probe beam throughout the crystal [Fig. 2(b)]. With a weak bias field, the intensity pattern induces a refractive index pattern so that waveguides with alternating strong and weak couplings are established. As illustrated in the simplified sketch of the SL [Fig. 2(c)], the SB corresponds to a shallow gap separating the strongly coupled waveguides, while the WB corresponds to a deep gap separating the weakly coupled waveguides. To test the

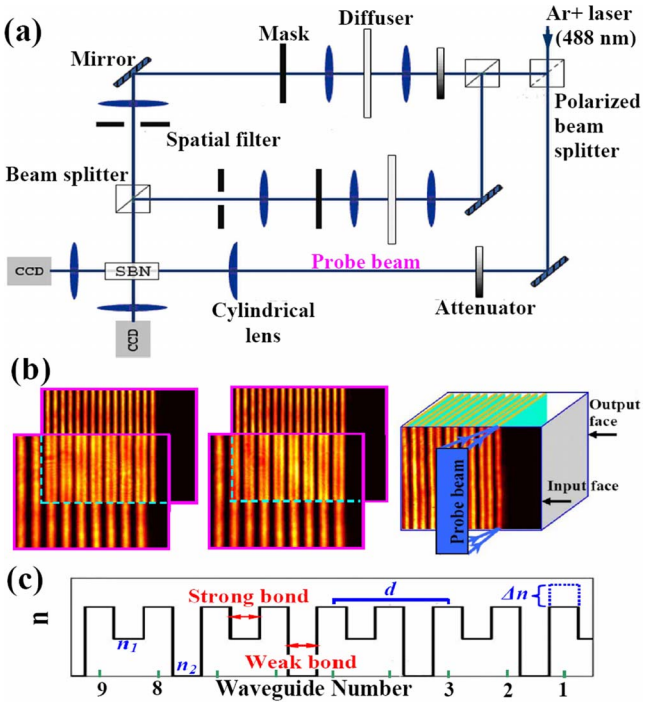

FIG. 2. (Color online) (a) Experimental setup for optical induction of photonic superlattices. (b) Configuration of superlattices terminated at strong (left) and weak (middle) bonds by superimposing two simple lattices of different periods (top and bottom) appropriately. The right panel is a three-dimensional (3D) rendering of a superlattice imprinted in a photorefractive crystal by optical induction. (c) Illustration of a simplified superlattice structure used for our theoretical analysis.

properties of wave propagation along different interfaces, an extraordinarily polarized probe beam is sent into the surface waveguide channel and its intensity pattern and phase structure are monitored with an imaging lens, a reference plane wave, and a charge coupled device (CCD) camera. So far, two different techniques have been used for optical induction of SLs [19,25].

We focus on beam propagation along the interface of the SL terminated at a SB because linear localization cannot occur at the interface of the SL terminated at a WB (as shown in our previous work [19]). Reconfiguration of the induced SL interface makes it possible to demonstrate different surface states shown in Fig. 3. In particular, the unique intensity and phase profile of the output probe beam [Fig. 3(b)] observed at the SB terminating surface waveguide without additional perturbation represent the characteristic signature of the SSs [19]. This linear surface confinement differs from the TSs previously observed in optics [10] as well as those recently observed with binary and other specially designed waveguide arrays [26,27]. Moreover, by intentionally introducing an index perturbation on the surface waveguide, we can demonstrate the transitions between TSs and SSs. The perturbation is created using two methods: one is to make the surface waveguide itself weaker than all the other waveguides by fine tuning the spatial filtering (linear scheme) and the other is to employ the nonlinearity of the probe beam to increase the surface waveguide index in the

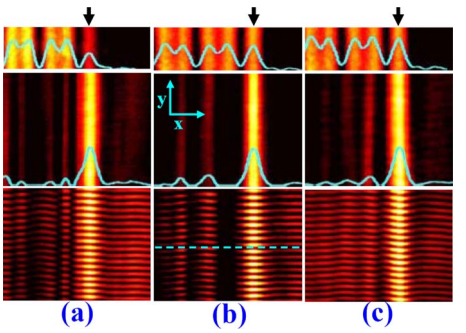

FIG. 3. (Color online) Experimental output results of the transition from linear Tamm-like to linear Shockley-like and to nonlinear Tamm-like surface states. The probe beam enters the first waveguide (shown with arrow) of the superlattice. (a) Linear Tamm-like state due to a negative surface defect. (b) Linear Shockley-like state at the surface without any perturbation. (c) Nonlinear Tamm-like state due to a self-induced positive surface defect. Top two rows: transverse intensity patterns of superlattice and output probe beams. Bottom row: phase measurement by interference between the output probe beam and a tilted plane wave.

otherwise ideal surface (nonlinear scheme). In both cases, localization of the probe beam at the surface is achieved, giving rise to linear and nonlinear TSs. Should the surface perturbation be minimized or removed, reappearance of the SS is observed. Typical experimental results of such transitions under different surface conditions are shown in Fig. 3, where Figs. 3(a) shows a *linear* TS obtained with a weakened surface waveguide (i.e., $\Delta n<0$, similar to a negative defect). Such a Tamm-like surface state has an evanescently decaying intensity profile and a characteristic "staggered" phase structure similar to that of surface gap solitons [14,15] but quite different from that of the Shockley-like surface state shown in Fig. 3(b). On the other hand, when the SL has no inherent surface perturbation, a positive surface defect ($\Delta n>0$) can be induced using nonlinear self-focusing of the probe beam at high power. This in turn leads to observation of a *nonlinear* TS as shown in Fig. 3(c), corresponding to that illustrated in Fig. 1(e). The in-phase relation in the "tail" of the surface mode shown in Fig. 3(c) is in sharp contrast to the results of Figs. 3(a) and 3(b). These experimental results provide direct evidence of transitions from linear TSs to linear SSs and to nonlinear TSs, as corroborated by our theoretical analysis below.

We now proceed with the theoretical study of wave propagation in a finite array of N identical, single-mode waveguides with alternating strong and weak couplings corresponding to SB and WB illustrated in Fig. 2(c). In terms of coupled-mode theory [28], the normalized amplitude of the electric field E_n localized in the nth waveguide can be found from the following set of nonlinear differential equations:

$$i\frac{d}{dz}E_1 + \alpha_1 E_1 + \beta_1 E_2 + \gamma|E_1|^2 E_1 = 0,$$

$$i\frac{d}{dz}E_{2n} + \alpha_{2n} E_{2n} + \beta_1 E_{2n-1} + \beta_2 E_{2n+1} + \gamma|E_{2n}|^2 E_{2n} = 0,$$

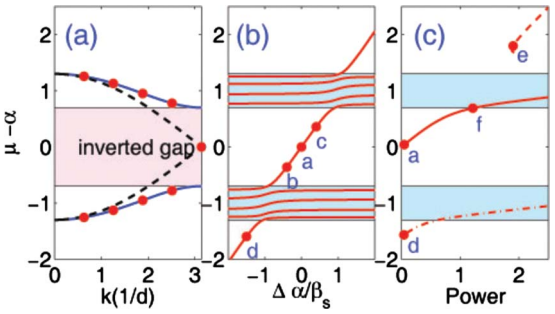

FIG. 4. (Color online) (a) The spectrum of the SL in the linear case: solid and dashed curves show the spectra of an infinite SL at $\beta_1=0.3\beta_2$ and $\beta_1=\beta_2$, respectively. Dots show the spectrum of a finite SL consisting of nine waveguides at $\beta_1=0.3\beta_2$. (b) Evolution of the spectrum of the nine-waveguide SL as a function of the surface perturbation. Solid curves show the modes of the finite SL. (c) Evolution of the surface modes shown in (b) as a function of the normalized power. Solid curve shows the Shockley mode. Dashed and dash-dotted curves show the nonlinear and linear Tamm modes, respectively. The shaded areas in (b) and (c) illustrate the allowed bands of the infinite SL, while the shaded area in (a) represents the inverted band gap.

$$i\frac{d}{dz}E_{2n+1}+\alpha_{2n+1}E_{2n+1}+\beta_2E_{2n}+\beta_1E_{2n+2}+\gamma|E_{2n+1}|^2E_{2n+1}=0, \quad (1)$$

where α_n is the linear propagation constant of the mode supported by the nth waveguide and $\beta_{1,2}$ are the two coupling constants corresponding to the weak and strong bonds. The waveguide array is terminated at a WB when $\beta_1=\beta_w$ but at a SB when $\beta_1=\beta_s$. The other parameters are the nonlinear coefficient γ, the longitudinal coordinate of propagation z, and the waveguide number n that runs from 1 to $N/2$ for even N or from 1 to $(N-1)/2$ for odd N. Accordingly, it is assumed that $E_n=0$ if $n>N$.

First, the linear regime ($\gamma=0$) of this system is examined. With an array of identical waveguides, $\alpha_n=\alpha$, the stationary modes of the waveguide arrays take the form $E_n(z)=\exp(i\mu z)E_n$, where μ is the Bloch-wave propagation constant which describes dispersion. For an infinite waveguide array, the solution to Eqs. (1) can be obtained by considering the SL as two simple sublattices. Thus, the values of E_n for each even and odd waveguides can be written as $a_n\exp(iknd)$ and $b_n\exp(iknd)$, respectively, where d is the lattice period [see Fig. 2(c)] and k is the Bloch vector in the direction perpendicular to the waveguides [17]. The dispersion relation of the infinite SL is defined as

$$\mu_{1,2}(k)=\alpha\pm\sqrt{\beta_1^2+\beta_2^2+2\beta_1\beta_2\cos(kd)}. \quad (2)$$

We can see that if both bonds are identical ($\beta_1=\beta_2\equiv\beta$), the dispersion relation becomes

$$\mu_{1,2}(k)=\alpha\pm\beta\cos(kd/2). \quad (3)$$

This is the spectrum of a simple lattice with a period of $d/2$. Once $\beta_1\neq\beta_2$, an inverted band gap of width $E_g=2|\beta_1-\beta_2|$ appears. In Fig. 4(a), we show the spectrum of an infinite SL with $\beta_1=0.3\beta_2$ by solid curves, while that of the simple lattice ($\beta_1=\beta_2$) by dashed curves. In the case of a SL with a finite number of waveguides, the dispersion relation can be found by numerically solving Eqs. (1). As an example, the dots in Fig. 4(a) show the spectrum of a SL consisting of nine waveguides with $\beta_1=0.3\beta_2$. When $\beta_1<\beta_2$, the SL is terminated by a SB [as shown in Fig. 2(c)]. As mentioned earlier for Fig. 1(d), in this case, there exists a surface mode in the middle of the inverted band gap. This localized surface mode appears only when the symmetry of the SB is broken at the surface and is not related to any perturbation on the surface waveguide. Accordingly, this must be classified as the Shockley surface mode [19] as it emerges from the crossing bands of a simple lattice with a period of $d/2$ and a Bloch vector $k_0=\pi/d$ [see dashed curves in Fig. 4(a)]. The phase of the Shockley mode is thus defined as

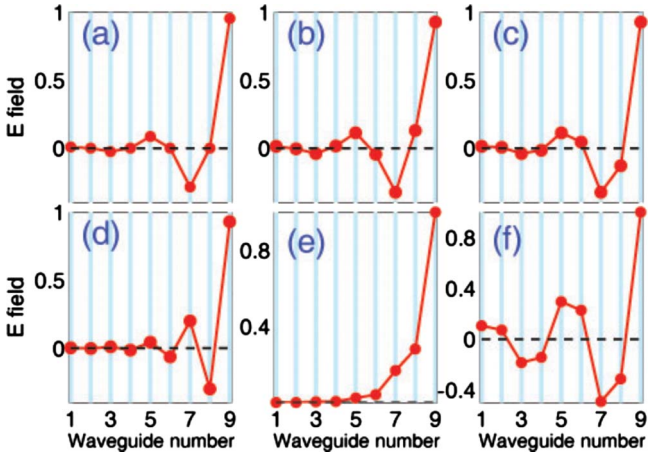

FIG. 5. (Color online) (a)–(f) Normalized field profiles of the surface modes from a nine-waveguide SL corresponding to marked points in Figs. 4(b) and 4(c). Notice the difference in phase structure and intensity patterns as observed in experiment. Vertical stripes illustrate the waveguides.

$$E_n^s\sim\exp(ik_0nd/2)=\exp(i\pi n/2). \quad (4)$$

So the fields in the first and third waveguides must have an out-of-phase relation [see also Fig. 5(a) above], which has been identified in our experiment for the unperturbed SL terminated at the SB [see Fig. 3(b)].

We further analyze the modes of the SL when perturbation on surface waveguide is introduced. In the linear regime, we still have $\gamma=0$, but now the linear propagation constant of the first waveguide changes so that $\alpha_1=\alpha-\Delta\alpha$, where $\Delta\alpha$ may be related to any surface perturbation such as an index change Δn as in our experiment or a change in the width of the surface waveguide. In Fig. 4(b), we show the SL mode spectrum with nine waveguides as a function of surface perturbation $\Delta\alpha$ with $\beta_1=0.3\beta_2$ and the mode profiles at marked points of Fig. 4(b) are presented in Fig. 5. When $\Delta\alpha=0$, the surface mode corresponds to the SS discussed above [located at point a in Fig. 4(b) and shown in Fig. 5(a)]. When $\Delta\alpha>\beta_s+\beta_w$, the surface mode shifts from the middle inverted gap to an ordinary gap [see point d in Figs. 4(b) and 5(d)] and shown intuitively in Fig. 1(e). (Note that in the case of the SB-terminated SL, $\beta_s=\beta_2$.) Since this surface mode ap-

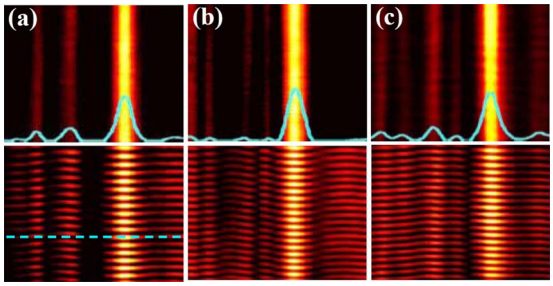

FIG. 6. (Color online) Experimental observation of a (a) linear "perfect" Shockley-like surface state and [(b) and (c)] two "deformed" Shockley-like surface states corresponding to those [(a)–(c)] in Figs. 4(b) and Fig. 5. Top row: transverse intensity patterns of the output probe beam. Bottom row: phase measurement by interference between the probe beam and a tilted plane wave.

pears only when the surface perturbation exceeds a critical value, it must be considered as a Tamm-like surface mode. The staggered phase structure [14,15,17] of this mode shown in Fig. 5(d) agrees with our experimental observation shown in Fig. 3(a).

In addition to the Tamm-like surface mode obtained at a threshold value of the surface perturbation, there are other types of linear surface modes at a slightly positive or negative surface index perturbation [see points b and c in Figs. 4(b), 5(b), and 5(c)]. The formation of such surface modes requires no threshold perturbation and they can exist even at an infinitely small perturbation. In fact, such surface modes still reside in the inverted band gap and have the same origin as Shockley-like states. We thus name these surface states as deformed Shockley-like states. Notice that their phase structures are different from those of perfect SSs or TSs. Two examples are shown in Fig. 5: an in-phase relationship between the first two waveguides and an out-of-phase relationship between the second and third waveguides as shown in Fig. 5(b); an out-of-phase relationship between the first two waveguides and an in-phase relationship between the second and third waveguides as shown in Fig. 5(c). All these subtle phase characteristics have been clearly observed in our experiments (Fig. 6), when a small negative or positive surface defect was introduced. In fact, perfect SSs from an ideal unperturbed surface [as shown in Figs. 3(b) and 6(a)] are difficult to achieve in our experiments and what we often observe are the deformed SSs shown in Figs. 6(b) and 6(c).

The *nonlinear* case ($\gamma \neq 0$) not only provides a better explanation for experimental observation in Fig. 3(c), but also provides a clear picture for the transition between SSs and TSs. The solution of the nonlinear system for N waveguides can be found numerically for any given value of μ. In Fig. 4(c), we show the evolution of Shockley-like (solid curve) and Tamm-like (dashed and dash-dotted curves) surface modes with increasing power $P=\Sigma_n|E_n|^2$. We can see that the SSs can exist even in the nonlinear regime, representing the nonlinear Shockley-like states. These Shockley states merge into the allowed band at $P=1.2$ [see point f in Fig. 4(c)] and then they turn into unstable modes due to radiation to the continuum spectrum. As the power further increases, the nonlinear Tamm-like modes appear from the upper band gap [see dashed curve in Fig. 4(c)]. These are the in-phase surface solitons that have been previously demonstrated with self-focusing nonlinearity at a threshold power [13,15,16]. The dash-dotted curve in Fig. 4(c) represents the nonlinear Tamm-like surface modes with "staggered" phase structures, as observed in experiment with self-defocusing nonlinearity [14,15]. As shown in Fig. 4(b), these modes also appear in the linear regime when $\Delta\alpha > \beta_s$. In the nonlinear case, these modes move up and also merge into the allowed band and become unstable as the power increases. The field profiles for the points e (nonlinear Tamm states) and f (nonlinear deformed Shockley states) are plotted in Figs. 5(e) and 5(f), respectively. The experimental demonstration of linear SSs to nonlinear TSs by increasing the beam power is shown in Figs. 3(b) and 3(c). Clearly, our theoretical results are in good agreement with our experimental observations. Finally, we would also like to mention that the field profiles of the linear surface modes in Figs. 5(a)–5(d) as well as the evolution of the spectrum shown in Fig. 4(b) are in good agreement with the results obtained recently with the transfer-matrix approach [19]. The consistency of the results from the coupled-mode theory and the transfer-matrix approach substantiates our theoretical analysis.

In conclusion, we have successfully demonstrated linear optical Shockley-like surface states and transitions between Shockley-like and Tamm-like surface states in light-induced photonic superlattices. We found that the Shockley-like states exist only when the superlattices are terminated at a strong bond. In addition, to reveal the characteristics of linear Shockley-like states, we have also demonstrated linear and nonlinear deformed Shockley-like states and transitions between linear and nonlinear surface states. Our results will certainly prove to be relevant to linear and nonlinear surface phenomena in other systems beyond optics.

This work was supported by NSF, USAFOSR, and the 973 Program.

[1] I. E. Tamm, Phys. Z. Sowjetunion **1**, 733 (1932).
[2] W. Shockley, Phys. Rev. **56**, 317 (1939).
[3] W. T. Sommer, Phys. Rev. Lett. **12**, 271 (1964); T. R. Brown and C. C. Grimes, *ibid.* **29**, 1233 (1972).
[4] A. A. Maradudin and G. I. Stegeman, in *Surface Phonons*, edited by W. Kress *et al.* (Springer-Verlag, Berlin, 1991).
[5] W. L. Barnes *et al.*, Nature (London) **424**, 824 (2003).
[6] H. Cercellier *et al.*, Phys. Rev. B **70**, 193412 (2004); C. Tiusan *et al.*, Phys. Rev. Lett. **93**, 106602 (2004).
[7] M. Pessa *et al.*, Phys. Rev. Lett. **47**, 1223 (1981); S. D. Kevan, *ibid.* **50**, 526 (1983).
[8] H. Ohno *et al.*, Phys. Rev. Lett. **64**, 2555 (1990); T. Miller *et al.*, *ibid.* **68**, 3339 (1992).
[9] A. Sommerfeld, Ann. Phys. **303**, 233 (1899); J. Zenneck, *ibid.*

328, 846 (1907); D. Kossel, J. Opt. Soc. Am. **56**, 1434 (1966).
[10] P. Yeh *et al.*, J. Opt. Soc. Am. **67**, 423 (1977); P. Yeh and A. Yariv, Appl. Phys. Lett. **32**, 104 (1978).
[11] A. D. Boardman *et al.*, in *Nonlinear Surface Electromagnetic Phenomena*, edited by H. E. Ponath and G. I. Stegeman (North-Holland, Amsterdam, 1991); F. Lederer *et al.*, Opt. Commun. **99**, 95 (1993); D. Mihalache *et al.*, Prog. Opt. **27**, 229 (1989); N. N. Akhmediev *et al.*, Sov. Phys. JETP **61**, 62 (1985).
[12] K. G. Makris *et al.*, Opt. Lett. **30**, 2466 (2005); **31**, 2774 (2006).
[13] S. Suntsov *et al.*, Phys. Rev. Lett. **96**, 063901 (2006).
[14] C. R. Rosberg *et al.*, Phys. Rev. Lett. **97**, 083901 (2006); A. Siviloglou *et al.*, Opt. Express **14**, 5508 (2006); E. Smirnov *et al.*, Opt. Lett. **31**, 2338 (2006).
[15] X. Wang *et al.*, Phys. Rev. Lett. **98**, 123903 (2007); Opt. Lett. **33**, 1240 (2008).
[16] A. Szameit *et al.*, Phys. Rev. Lett. **98**, 173903 (2007); Opt. Lett. **34**, 797 (2009).
[17] Y. V. Kartashov *et al.*, Phys. Rev. Lett. **96**, 073901 (2006).
[18] N. Malkova, C. Ning, Phys. Rev. B **73**, 113113 (2006); **76**, 045305 (2007).
[19] N. Malkova *et al.*, Opt. Lett. **34**, 1633 (2009); X. Wang, N. Malkova, I. Hromada, G. Bryant, and Z. Chen, Optical Shockley-like surface states in light-induced superlattices, in *Conference on Lasers and Electro-Optics*, OSA Technical Digest (CD) (Optical Society of America, 2008), paper JTuA124.
[20] I. L. Garanovich *et al.*, Phys. Rev. Lett. **100**, 203904 (2008); A. Szameit *et al.*, *ibid.* **101**, 203902 (2008).
[21] N. K. Efremidis *et al.*, Phys. Rev. E **66**, 046602 (2002).
[22] J. W. Fleischer *et al.*, Nature (London) **422**, 147 (2003).
[23] Z. Chen and K. McCarthy, Opt. Lett. **27**, 2019 (2002); H. Martin *et al.*, Phys. Rev. Lett. **92**, 123902 (2004).
[24] Z. Chen and J. Yang, in *Nonlinear Optics and Applications*, edited by H. Abdeldayem and D. O. Frazier (Research Signpost, Kerala, India, 2007).
[25] P. Rose *et al.*, J. Phys. D **41**, 224004 (2008).
[26] R. Morandotti *et al.*, Opt. Lett. **29**, 2890 (2004); M. I. Molina *et al.*, *ibid.* **31**, 2332 (2006).
[27] S. Suntsov *et al.*, Opt. Express **15**, 4663 (2007); A. Szameit *et al.*, Opt. Lett. **33**, 1132 (2008).
[28] D. N. Christodoulides and R. I. Joseph, Opt. Lett. **13**, 794 (1988); Y. S. Kivshar, *ibid.* **18**, 1147 (1993).